Water Production in Comets 2001 Q4 (NEAT) and 2002 T7 (LINEAR) Determined from SOHO/SWAN Observations

M.R. Combi, J.T.T. Mäkinen, Jean-Loup Bertaux, Y. Lee, Eric Quémerais

The Astronomical Journal, 137:4734–4743, 2009 June doi:10.1088/0004-6256/137/6/4734

WATER PRODUCTION IN COMETS 2001 Q4 (NEAT) AND 2002 T7 (LINEAR) DETERMINED FROM *SOHO*/SWAN OBSERVATIONS

M. R. Combi[1], J. T. T. Mäkinen[2], J.-L. Bertaux[3], Y. Lee[1], and E. Quémerais[3]
[1] Department of Atmospheric, Oceanic and Space Sciences, University of Michigan, 2455 Hayward Street, Ann Arbor, MI 48109-2143, USA; mcombi@umich.edu
[2] Finnish Meteorological Institute, Box 503, SF-00101 Helsinki, Finland
[3] Centre National de la Recherche Scientifique, Service d'Aéronomie, BP3, 91371 Verrières le Buisson Cedex, France
Received 2008 November 25; accepted 2009 March 9; published 2009 April 27

ABSTRACTS

The SWAN all-sky camera on the *Solar and Heliospheric Observatory* (*SOHO*) spacecraft detected the hydrogen Lyman-alpha (Lyα) comae of comets 2001 Q4 NEAT and 2002 T7 LINEAR for large portions of their perihelion apparitions in 2003 and 2004. C/2001 Q4 NEAT was observed from 2003 September 14 through 2004 November 2, covering heliocentric distances from 3.23 AU before perihelion to 2.75 AU after, and C/2002 T7 LINEAR was observed from 2003 December 4 through 2004 August 6, covering heliocentric distances from 2.52 AU before perihelion to 2.09 AU after. We combined the full set of comet specific and full-sky observations and used our time-resolved model (TRM), which enables us to extract continuous values of the daily-average value of the water production rate throughout most of this entire period. The average power-law fit to the production rate variation of C/2001 Q4 NEAT with heliocentric distance, r, gives $3.5 \times 10^{29}\, r^{-1.7}$ and that for C/2002 T7 LINEAR gives $4.6 \times 10^{29}\, r^{-2.0}$. Both comets show roughly a factor of 2 asymmetry in activity about perihelion, being more active before perihelion. C/2001 Q4 NEAT showed a production rate outburst about 30 days before perihelion (2004 April 15) and then a large extended increase above the nominal trend from 50 to 70 days after perihelion (2004 July 5–July 25).

Key words: comets: general – comets: individual (C/2001 Q4 (NEAT), C/2002 T7 (LINEAR)) – Oort Cloud

1. INTRODUCTION

Being stationed at the L1 Lagrange point 1.5 million km in front of the Earth, the *Solar and Heliospheric Observatory* (*SOHO*) spacecraft has been well positioned for 13 years to obtain continuous temporal coverage of the Sun and solar wind. The *SOHO* Solar Wind Anisotropies (SWAN) camera, makes all-sky Lyman-alpha (Lyα) images of the hydrogen distribution in the interplanetary medium (IPM), typically in the brightness range of 500–1000 Rayleighs, providing a global picture of the solar wind, which shapes the hydrogen distribution by charge impact ionization (Bertaux et al. 1997).

Because solar ultraviolet radiation dissociates cometary water and its byproduct OH, producing two hydrogen atoms per molecule, comets are surrounded by a large atomic hydrogen coma, which being illuminated by solar Lyα photons at 1215.7 Å, presents a useful target for monitoring the water production rate in comets. Obtaining accurate water production rates in comets is particularly important because water is usually the most abundant parent gas species in the coma, controlling the overall activity, because measurements of all other species are compared to it for compositional interpretation, and because of the crucial role of comets in the larger issue of the origin of the solar system. Furthermore, we have developed a method of simultaneously analyzing sets of SWAN images, usually recorded a few times per week, to extract daily average values of the water production rate by the nucleus (Mäkinen & Combi 2005). Using the extracted daily-average values we have compared with various complementary data sets (Combi et al. 2005, 2008) and found reasonable agreement with both long-term and short-term variations of the cometary water production, including large outbursts.

This analysis procedure combines and extends the best and necessary parts of the syndyname approaches of Keller and Meier (1976), the vectorial model of Festou (1981), and a parameterized version of the collisional physics Monte Carlo models of Combi and Smyth (1988) into a reasonably computationally fast tool for analyzing both single SWAN images as well as a series of the wide-field observations of the H Lyα coma. The model builds up time-tagged, sky-plane basis functions of H Lyα for the times and various locations within a whole set of SWAN images that correspond to a certain production rate of water molecules from the nucleus. By employing a standard inversion technique (the Singular Value Decomposition), the time-resolved model (TRM) can be used to calculate either an average production rate for a single image or to deconvolve a whole set of images into water production rates at some desired time-resolution between many images (Mäkinen & Combi 2005). Given the field of view of SWAN and photochemical lifetimes of water and OH, usually daily-average values of the water production rate at the nucleus can be extracted from a series of images taken at a rate of 2–4 per week. Using this procedure we were able to analyze a large set of Lyα images of comet 1996 B2 Hyakutake and resolve three major outbursts including the well-known 1996 March 19 outburst. We have since used the TRM for several other comets for both single-image production rates (Mäkinen et al. 2007; Neugebauer et al. 2007) and daily averages (Combi et al. 2008).

Here, we present the results of a TRM analysis of more than a year of SWAN observations in 2003 and 2004 of comets C/2001 Q4 (NEAT), hereafter referred to as Q4, and eight months of observations of C/2002 T7 (LINEAR), hereafter referred to as T7. These comets were discovered by two of the near Earth object (NEO) survey telescopes while they were quite far from the Sun in 2001 and 2002, and both were anticipated and well planned observationally. Comet 2001 Q4 NEAT was observed by SWAN from 2003 September 14 through 2004 November 2, covering heliocentric distances from 3.23 AU before perihelion to 2.75 AU after. Comet 2002 T7 LINEAR was observed from 2003 December 4 through 2004 August 6, covering heliocentric distances from 2.52 AU before perihelion to 2.09 AU after. With the TRM we calculated both single-image

Table 1
C/2002 T7 LINEAR: Observational Circumstances and Single-Image Water Production Rates

ΔT (days)	r (AU)	Δ (AU)	g (s^{-1})	Q (10^{28} s^{-1})	δQ (10^{28} s^{-1})
−141.379	2.515	1.602	0.001716	8.981	0.02
−140.323	2.501	1.596	0.001715	4.206	0.05
−139.268	2.487	1.590	0.001714	13.17	0.01
−138.212	2.473	1.585	0.001714	6.722	0.03
−136.096	2.444	1.576	0.001713	15.72	0.01
−128.704	2.344	1.568	0.001709	15.97	0.01
−127.649	2.329	1.569	0.001708	23.83	0.01
−126.593	2.315	1.571	0.001707	10.16	0.02
−125.537	2.300	1.573	0.001707	18.62	0.01
−124.481	2.286	1.576	0.001706	14.64	0.01
−123.425	2.271	1.580	0.001706	15.02	0.01
−122.368	2.257	1.583	0.001705	16.55	0.007
−121.313	2.242	1.588	0.001705	20.46	0.007
−120.257	2.228	1.592	0.001725	16.33	0.006
−119.201	2.213	1.598	0.001724	16.82	0.01
−118.145	2.198	1.603	0.001724	15.75	0.007
−106.606	2.036	1.685	0.001718	21.43	0.008
−106.289	2.031	1.687	0.001718	18.98	0.002
−104.601	2.007	1.702	0.001717	23.05	0.008
−102.792	1.981	1.717	0.001716	25.80	0.006
−100.498	1.948	1.738	0.001715	32.26	0.007
−98.689	1.922	1.754	0.001734	30.57	0.006
−96.887	1.896	1.770	0.001733	27.77	0.007
−95.078	1.869	1.786	0.001733	28.16	0.007
−92.787	1.836	1.807	0.001731	25.45	0.008
−90.986	1.809	1.823	0.001730	28.79	0.008
−89.177	1.783	1.839	0.001730	27.83	0.007
−86.883	1.749	1.858	0.001728	29.59	0.009
−85.073	1.722	1.873	0.001727	28.81	0.009
−57.790	1.307	2.007	0.001736	54.74	0.007
−54.265	1.252	2.007	0.001735	82.21	0.001
−53.512	1.240	2.006	0.001734	58.37	0.007
−51.882	1.215	2.004	0.001733	47.94	0.002
−50.514	1.194	2.001	0.001733	54.89	0.007
−48.716	1.166	1.996	0.001732	56.29	0.007
−46.572	1.133	1.988	0.001731	60.62	0.007
−43.586	1.087	1.973	0.001730	56.36	0.008
−41.774	1.059	1.961	0.001729	72.35	0.009
−39.641	1.026	1.946	0.001728	83.77	0.007
−7.637	0.637	1.354	0.001472	174.6	0.002
−6.138	0.629	1.308	0.001464	118.0	0.009
−4.717	0.623	1.262	0.001450	128.7	0.001
−3.923	0.621	1.236	0.001444	119.7	0.007
6.320	0.630	0.866	0.001422	74.91	0.004
7.375	0.635	0.826	0.001425	93.47	0.003
9.814	0.651	0.732	0.001443	96.70	0.003
13.148	0.678	0.605	0.001468	66.05	0.003
15.919	0.705	0.502	0.001486	69.78	0.003
18.292	0.731	0.420	0.001506	55.07	0.003
36.424	0.978	0.498	0.001577	23.83	0.004
39.438	1.023	0.605	0.001591	26.77	0.005
41.251	1.051	0.671	0.001590	23.67	0.005
43.396	1.084	0.750	0.001589	22.44	0.007
67.583	1.458	1.619	0.001582	9.331	0.02
69.250	1.483	1.676	0.001582	10.40	0.02
71.250	1.514	1.743	0.001581	6.999	0.03
74.250	1.559	1.842	0.001581	8.441	0.03
75.286	1.575	1.876	0.001580	9.533	0.03
76.342	1.591	1.910	0.001580	11.46	0.03
84.480	1.713	2.164	0.001564	13.18	0.03
86.855	1.748	2.236	0.001563	5.425	0.06
88.605	1.774	2.288	0.001563	11.17	0.03
89.479	1.787	2.313	0.001563	7.181	0.008
95.598	1.877	2.487	0.001561	8.706	0.009
100.849	1.953	2.629	0.001546	8.373	0.06
101.465	1.962	2.645	0.001546	5.376	0.01
102.599	1.978	2.674	0.001546	9.510	0.04
105.474	2.019	2.748	0.001545	12.67	0.05

Notes.
ΔT: time from perihelion 2004 April 23.0623, in days.
r : heliocentric distance (AU).
Δ: geocentric distance (AU).
g: solar Lyα g-factor (photons s^{-1}).
Q: water production rate (10^{28} s^{-1}).
δQ: 1σ uncertainty (10^{28} s^{-1}).

production rates as well as deconvolved daily average values, covering the activity of Q4 and T7 for long continuous intervals of time. We examine the pre- and post-perihelion activity and the variation of activity with heliocentric distance. We also compare the water production rates with published results of water production rate from observations of water and its other photodissociation products. Finally, we discuss the variation with heliocentric distance with the expanding set of comets observed in this manner with SWAN.

2. TRM ANALYSIS RESULTS

Tables 1 and 2 give the observational circumstances, and Figures 1 and 2 show the entire set of single-image water production rates for T7 and Q4, respectively. The production rate values at the time the image was obtained are extracted assuming only the long-term heliocentric distance dependent variation of water production rate within the image. It is clear that both of these comets were just over a factor of 2 more productive at comparable heliocentric distances before perihelion compared to after. On the other hand, the overall slopes of the variations before and after perihelion are similar for each comet. The average power-law fit to the production rate variation of Q4 gives 3.5×10^{29} $r^{-1.7}$ and that for T7 gives 4.6×10^{29} $r^{-2.0}$. Please note the power-law fits do include all the data as given, including any short-term variations such as outbursts. One advantage of SWAN having both wide and continuous coverage is that we can to a certain extent average over short-term activity variations.

Tables 3 and 4 and Figures 3 and 4 give the TRM daily-average deconvolved water production rates for T7 and Q4, respectively. For both comets there are sporadic gaps in the daily-average coverage, normally when the comet is too close to bright stars, e.g., near the galactic equator. There are not many water production rate values for these comets available in the published literature yet, but those that are available are plotted with the SWAN results. The Odin microwave observations (Biver et al. 2007) agree quite well with the T7 results. Those for Q4 are somewhat below the SWAN results. Preliminary results from infrared observations of water (Anderson et al. 2008) are in excellent agreement for T7. Their one value for Q4 is almost a factor of two above the SWAN values. J. Crovisier et al. (2009, in preparation) have provided preliminary results of OH 18 cm observations of Q4 from Nançay. This range of differences in consistency is similar to those found between SWAN results and other methodologies (water in the IR, OH in near UV and radio, etc.) in the SWAN results for the five moderately bright comets from 1999 to 2001 (Combi et al. 2008).

Table 2
C/2001 Q4 NEAT: Observational Circumstances and Single-Image Water Production Rates

ΔT (days)	r (AU)	Δ (AU)	g (s^{-1})	Q (10^{28} s^{-1})	δQ (10^{28} s^{-1})
−212.872	3.233	2.975	0.001674	1.525	0.13
−208.976	3.189	2.950	0.001672	1.850	0.022
−206.326	3.159	2.935	0.001671	2.236	0.089
−192.309	2.997	2.865	0.001678	3.480	0.054
−175.881	2.805	2.802	0.001669	4.135	0.067
−173.770	2.780	2.794	0.001668	4.585	0.052
−172.725	2.768	2.790	0.001667	2.847	0.080
−171.669	2.756	2.787	0.001666	6.978	0.036
−168.507	2.718	2.775	0.001665	9.365	0.024
−166.406	2.693	2.767	0.001664	7.121	0.036
−165.355	2.681	2.763	0.001663	4.932	0.045
−163.243	2.656	2.755	0.001662	6.446	0.035
−162.197	2.643	2.750	0.001662	3.790	0.059
−161.141	2.630	2.746	0.001661	4.699	0.050
−159.035	2.605	2.737	0.001660	2.550	0.089
−157.979	2.593	2.733	0.001659	3.078	0.081
−156.933	2.580	2.728	0.001658	4.907	0.053
−151.659	2.517	2.704	0.001656	8.876	0.027
−149.557	2.491	2.693	0.001655	8.606	0.029
−148.506	2.479	2.688	0.001654	5.903	0.039
−147.450	2.466	2.682	0.001654	7.778	0.030
−146.395	2.453	2.677	0.001653	11.17	0.024
−145.348	2.440	2.671	0.001653	8.664	0.030
−144.292	2.427	2.665	0.001669	6.619	0.033
−143.237	2.415	2.659	0.001669	10.03	0.027
−142.186	2.402	2.653	0.001668	9.701	0.026
−141.130	2.389	2.646	0.001668	6.309	0.042
−129.546	2.247	2.565	0.001662	9.312	0.017
−127.527	2.223	2.549	0.001661	12.73	0.013
−125.714	2.200	2.533	0.001660	14.02	0.013
−123.408	2.172	2.513	0.001659	12.64	0.015
−121.596	2.150	2.496	0.001658	16.90	0.011
−119.783	2.127	2.479	0.001657	18.47	0.0097
−117.970	2.105	2.461	0.001656	16.59	0.011
−115.665	2.076	2.437	0.001655	18.64	0.0090
−113.852	2.054	2.418	0.001654	18.93	0.0086
−112.039	2.031	2.397	0.001653	18.28	0.0088
−109.734	2.003	2.371	0.001652	18.48	0.0085
−107.921	1.980	2.349	0.001651	20.89	0.0079
−105.935	1.956	2.324	0.001650	83.74	0.067
−103.435	1.925	2.292	0.001649	24.60	0.0014
−102.935	1.918	2.285	0.001649	25.15	0.0056
−102.018	1.907	2.273	0.001648	27.57	0.0017
−100.268	1.885	2.249	0.001648	24.11	0.015
−99.116	1.871	2.233	0.001647	27.12	0.0014
−98.643	1.865	2.226	0.001647	30.56	0.0050
−96.742	1.842	2.198	0.001646	25.58	0.0013
−95.643	1.828	2.182	0.001646	32.32	0.0053
−93.496	1.801	2.149	0.001645	27.68	0.0058
−91.826	1.781	2.123	0.001644	27.02	0.0012
−89.452	1.751	2.085	0.001643	32.16	0.0011
−88.351	1.738	2.067	0.001642	27.45	0.0053
−86.204	1.711	2.030	0.001642	29.40	0.0054
−84.058	1.685	1.993	0.001641	29.62	0.0052
−81.058	1.648	1.938	0.001639	32.73	0.0050
−80.147	1.637	1.921	0.001639	34.20	0.00090
−78.911	1.622	1.898	0.001638	32.57	0.0047
−77.243	1.602	1.866	0.001638	39.66	0.00079
−76.765	1.596	1.857	0.001637	31.73	0.0047
−74.868	1.573	1.819	0.001620	37.35	0.00089
−73.765	1.560	1.797	0.001619	35.53	0.0046
−71.954	1.538	1.760	0.001618	38.91	0.0047
−69.808	1.512	1.716	0.001617	40.07	0.0042
−66.808	1.476	1.651	0.001616	43.95	0.0033
−64.995	1.455	1.611	0.001615	37.96	0.0034

Table 2
(Continued)

ΔT (days)	r (AU)	Δ (AU)	g (s^{-1})	Q (10^{28} s^{-1})	δQ (10^{28} s^{-1})
−60.335	1.401	1.505	0.001599	45.97	0.0059
−59.827	1.395	1.493	0.001599	38.34	0.0033
−58.014	1.374	1.451	0.001598	37.54	0.0033
−55.868	1.350	1.399	0.001597	35.70	0.0036
−52.869	1.317	1.326	0.001596	28.57	0.0057
−51.056	1.297	1.281	0.001581	26.87	0.0037
−39.149	1.175	0.970	0.001549	30.09	0.0044
−37.797	1.162	0.933	0.001548	32.97	0.00077
−36.246	1.148	0.891	0.001534	29.67	0.0041
−34.895	1.135	0.855	0.001534	34.62	0.00069
−34.090	1.128	0.833	0.001534	31.93	0.0036
−32.520	1.115	0.790	0.001521	31.69	0.00069
−31.090	1.103	0.752	0.001521	31.26	0.0029
−30.506	1.098	0.736	0.001520	33.27	0.00062
−28.954	1.085	0.694	0.001508	29.10	0.0029
−26.809	1.069	0.637	0.001496	27.71	0.0028
−25.357	1.058	0.599	0.001496	54.85	0.0014
−17.220	1.008	0.409	0.001460	28.47	0.0014
−16.121	1.002	0.388	0.001460	29.61	0.0016
−13.982	0.993	0.355	0.001452	40.08	0.00089
−13.634	0.991	0.351	0.001452	28.82	0.0018
−11.607	0.983	0.331	0.001445	31.31	0.00055
−7.494	0.971	0.328	0.001432	37.63	0.0026
−5.109	0.966	0.350	0.001423	36.84	0.0027
−1.163	0.962	0.414	0.001416	30.22	0.0021
1.476	0.962	0.471	0.001416	25.30	0.0026
3.288	0.964	0.513	0.001413	20.95	0.0033
5.290	0.966	0.563	0.001411	22.35	0.0032
8.315	0.973	0.640	0.001409	22.10	0.0038
10.139	0.978	0.688	0.001409	22.28	0.0040
13.403	0.990	0.775	0.001411	18.73	0.0048
16.422	1.004	0.855	0.001413	18.64	0.0052
18.235	1.013	0.903	0.001415	19.12	0.0054
20.390	1.026	0.960	0.001420	19.64	0.0051
23.409	1.045	1.038	0.001426	16.93	0.0065
25.222	1.057	1.084	0.001432	16.40	0.0076
27.377	1.073	1.138	0.001439	16.61	0.0079
30.376	1.097	1.211	0.001447	15.88	0.0079
32.210	1.112	1.254	0.001447	16.14	0.0079
34.355	1.131	1.305	0.001455	14.38	0.0085
38.465	1.168	1.397	0.001463	11.90	0.12
44.663	1.229	1.528	0.001471	13.28	0.014
46.323	1.246	1.562	0.001481	14.94	0.014
48.323	1.267	1.601	0.001480	15.52	0.014
51.315	1.300	1.657	0.001480	14.92	0.015
52.364	1.311	1.677	0.001479	13.15	0.016
53.420	1.323	1.696	0.001490	16.28	0.015
54.475	1.334	1.714	0.001490	19.07	0.015
56.843	1.361	1.755	0.001489	20.74	0.012
58.593	1.381	1.785	0.001489	26.49	0.010
61.544	1.415	1.832	0.001499	29.83	0.010
63.911	1.442	1.869	0.001498	28.59	0.011
65.654	1.463	1.894	0.001498	25.41	0.012
66.575	1.474	1.908	0.001497	24.12	0.0023
72.639	1.546	1.990	0.001496	10.76	0.020
75.508	1.581	2.026	0.001495	10.62	0.021
77.875	1.609	2.054	0.001507	10.69	0.021
79.625	1.631	2.074	0.001507	9.974	0.023
80.575	1.642	2.084	0.001507	11.98	0.0040
82.494	1.666	2.105	0.001506	9.284	0.023
84.862	1.695	2.129	0.001506	9.804	0.023
86.606	1.716	2.146	0.001505	10.37	0.022
89.557	1.753	2.173	0.001505	8.652	0.025
91.932	1.782	2.194	0.001504	6.097	0.030
93.676	1.804	2.208	0.001504	7.022	0.029
96.460	1.838	2.230	0.001503	6.228	0.029

Table 2
(Continued)

ΔT (days)	r (AU)	Δ (AU)	g (s^{-1})	Q (10^{28} s^{-1})	δQ (10^{28} s^{-1})
100.050	1.883	2.256	0.001502	7.318	0.026
102.939	1.918	2.276	0.001502	7.179	0.030
105.314	1.948	2.291	0.001501	8.051	0.028
107.072	1.970	2.301	0.001501	7.483	0.027
109.951	2.005	2.317	0.001501	4.486	0.047
111.348	2.023	2.325	0.001500	3.959	0.057
120.780	2.139	2.369	0.001499	6.427	0.034
126.378	2.208	2.392	0.001497	7.562	0.029
138.835	2.361	2.437	0.001495	5.311	0.023
141.209	2.390	2.446	0.001495	4.109	0.031
147.704	2.469	2.469	0.001482	4.827	0.024
148.759	2.482	2.473	0.001482	3.344	0.034
151.877	2.519	2.486	0.001481	5.492	0.026
152.933	2.532	2.490	0.001481	3.500	0.035
153.988	2.545	2.494	0.001481	3.685	0.034
170.986	2.748	2.581	0.001478	4.170	0.025

Notes.
ΔT: time from perihelion 2004 May 15.97, in days.
r : heliocentric distance (AU).
Δ: geocentric distance (AU).
g: solar Lyα g-factor (photons s^{-1}).
Q: water production rate (10^{28} s^{-1}).
δQ: 1σ uncertainty (10^{28} s^{-1}).

3. DISCUSSION

Q4 is a dynamically new Oort Cloud comet (Biver et al. 2007). The pre-perihelion variation seen in Figure 2, unlike many of the SWAN comets, is not characterized by a uniform overall "straight line" slope as in the best-fit power law, but rather is steeper than the power law for $r > 2$ AU and somewhat more shallow for $r < 1.3$ AU. This is somewhat reminiscent of the seasonal variation resulting from an active spot seen in comet 19P/Borrelly and characterized by Schleicher et al. (2003). During most of the pre-perihelion period, roughly from 2.2 to 1.5 AU the production rate has a broad enhancement above the mean power-law distribution. There was then a very large production rate spike (outburst) about 30 days before perihelion. The general trend after perihelion follows the straight-line power-law slope (see Figure 2) closely, except for a large extended increase above the nominal trend from 50 to 70 days after perihelion. The fact that the largest production rate is before perihelion and that there is a rise in the production rate ~60 days after perihelion is also reflected in the visual light curve (Yoshida, 2008), which peaks about 2 weeks before perihelion and which has a definite shoulder in the post-perihelion leg.

T7 does not show any peculiar activity changes or outbursts beyond having larger production rates before perihelion than after. The visual light curve (Yoshida 2008), although overall larger before perihelion than after, is consistent with the water

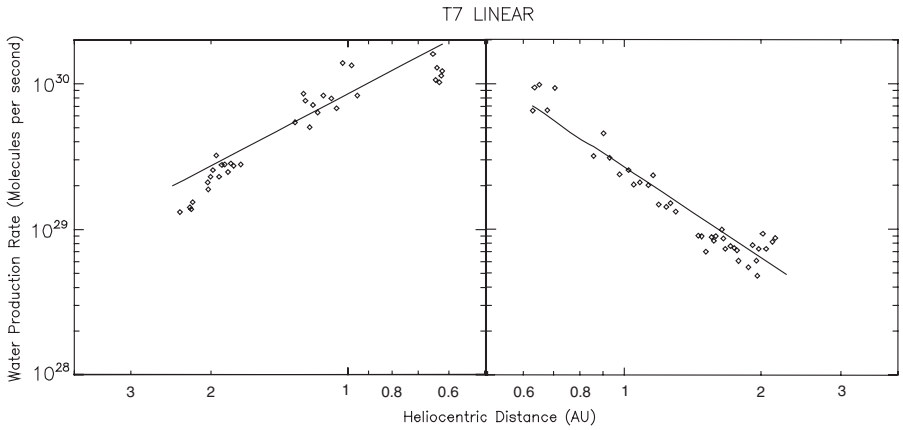

Figure 1. Single-image water production rate in C/2002 T7 (LINEAR) as a function of heliocentric distance. Shown as the points are the single-image water production rates determined from the SWAN images of the Lyα coma of comet C/2002 T7 (LINEAR). The straight lines give the best-fit power-law variations for the separate pre- (left) and post-perihelion (right) results, which are 8.4×10^{29} $r^{-1.6}$ and 2.7×10^{29} $r^{-2.1}$, respectively, in molecules s^{-1} with heliocentric distance, r, in AU.

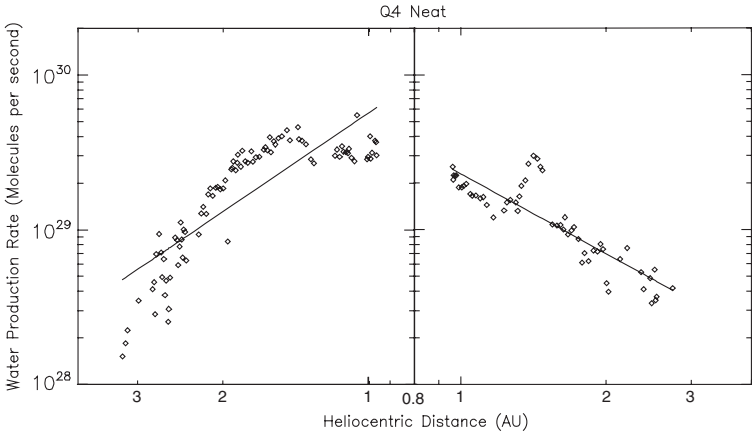

Figure 2. Single-image water production rate in C/2001 Q4 (NEAT) as a function of heliocentric distance. Shown as the points are the single-image water production rates determined from the SWAN images of the Lyα coma of comet C/2001 Q4 (NEAT). The straight lines give the best-fit power-law variations for the separate pre- (left) and post-perihelion (right) results, which are 5.8×10^{29} $r^{-2.2}$ and 2.3×10^{29} $r^{-1.7}$, respectively, in molecules s^{-1} with heliocentric distance, r, in AU.

Table 3
C/2002 T7 LINEAR: Deconvolved Daily-Average Water Production Rates

ΔT (days)	Q (10^{28} s^{-1})	δQ (10^{28} s^{-1})
−134.076	14.65	13
−133.076	14.28	13.
−132.076	15.19	11.
−131.076	16.76	11.
−130.076	18.27	9.1
−129.076	16.68	9.3
−128.076	18.78	6.8
−127.076	16.81	7.6
−126.076	17.37	5.0
−125.076	17.67	7.9
−124.076	19.17	4.8
−123.076	16.82	8.3
−122.076	17.25	4.9
−121.076	17.41	15.
−120.076	18.18	13.
−119.076	17.70	12.
−118.076	18.26	11.
−117.076	18.46	11.
−116.076	17.49	11.
−115.076	15.94	11.
−114.076	17.47	8.8
−113.076	19.60	7.9
−112.076	19.49	6.8
−111.076	20.20	6.6
−110.076	20.22	4.9
−109.076	22.50	7.2
−108.076	23.37	5.5
−107.076	24.26	8.3
−106.076	25.73	6.8
−105.076	26.36	9.5
−104.076	27.92	8.5
−103.076	27.05	9.8
−102.076	28.29	8.1
−101.076	26.56	10.
−100.076	27.14	7.8
−99.076	27.87	9.1
−98.076	28.81	6.0
−97.076	25.74	9.8
−96.076	27.53	12.
−95.076	27.67	11.
−94.076	27.41	8.4
−93.076	27.90	13.
−92.076	27.83	12.
−91.076	27.59	10.
−84.076	29.49	20.
−83.076	29.95	20.
−82.076	27.97	19.
−81.076	27.83	19.
−80.076	27.51	19.
−79.076	27.20	19.
−78.076	26.99	22.
−77.076	26.73	22.
−76.076	26.48	22.
−75.076	26.41	17.
−74.076	26.24	17.
−73.076	26.10	17.
−72.076	39.33	20.
−71.076	39.57	19.
−70.076	40.25	19.
−69.076	18.93	22.
−68.076	21.22	20.
−67.076	23.76	18.
−66.076	26.46	18.
−65.076	29.49	15
−64.076	32.70	14.
−63.076	38.64	14.

Table 3
(Continued)

ΔT (days)	Q (10^{28} s^{-1})	δQ (10^{28} s^{-1})
−62.076	42.30	12.
−61.076	45.48	12.
−60.076	50.14	21.
−59.076	51.26	18.
−58.076	53.41	14.
−57.076	40.87	15.
−56.076	38.89	11.
−55.076	34.71	4.3
−54.076	50.23	22.
−53.076	49.56	18.
−52.076	48.73	13.
−51.076	54.19	22.
−50.076	54.24	17.
−49.076	55.18	10.
−48.076	56.76	28.
−47.076	56.96	23.
−46.076	56.51	19.
−13.076	175.2	140
−12.076	129.8	66.
−11.076	107.5	24.
−10.076	96.99	10.
−9.076	104.1	1.4
−8.076	94.83	1.4
−4.076	82.60	24.
−3.076	88.77	32.
−2.076	71.10	19.
−1.076	58.58	11.
−0.076	59.23	7.5
0.924	56.11	3.8
1.924	49.38	2.1
2.924	47.40	0.56
3.924	54.86	0.31
4.924	90.89	1.9
5.924	71.60	1.9
6.924	85.70	1.0
7.924	116.3	1.5
8.924	53.32	3.1
9.924	52.28	1.3
10.924	58.67	0.96
11.924	59.30	1.4
12.924	60.04	0.51
13.924	64.08	0.55
29.924	26.47	6.7
30.924	27.11	6.8
31.924	26.78	5.3
32.924	25.45	2.1
33.924	25.08	1.2
34.924	27.14	3.1
35.924	27.66	2.0
36.924	30.64	2.2
37.924	36.92	1.3
38.924	22.43	0.68
54.924	14.72	7.3
55.924	14.22	7.0
56.924	5.144	6.5
57.924	5.540	6.3
58.924	5.922	5.8
59.924	6.391	5.4
60.924	6.819	4.9
61.924	7.441	4.6
62.924	8.096	5.6
63.924	8.973	4.7
64.924	12.61	7.1
65.924	11.65	5.5
66.924	9.834	5.3
67.924	8.340	2.8

Table 3
(Continued)

ΔT (days)	Q (10^{28} s^{-1})	δQ (10^{28} s^{-1})
68.924	9.281	6.8
69.924	9.404	6.6
70.924	9.840	5.8
73.924	9.731	9.7
74.924	9.905	8.6
75.924	10.26	8.5
76.924	11.59	7.4
77.924	10.64	7.5
78.924	11.22	7.5
79.924	9.691	8.9
80.924	8.535	8.5
81.924	8.882	7.9
82.924	9.000	7.0
83.924	9.371	6.9
84.924	8.577	5.4
85.924	8.148	4.0
91.924	8.216	7.4
93.924	8.942	8.2
94.924	8.801	8.0
95.924	8.330	6.7
96.924	7.965	5.7
97.924	7.421	4.0

Notes.
ΔT: time from perihelion 2004 April 23.06, in days
Q: water production rate (10^{28} s^{-1}).
δQ: 1σ uncertainty (10^{28} s^{-1}).

production and has its largest peak or a dust outburst about 30 days after perihelion. Such behavior is not seen in either the record of the single-image or the daily deconvolved water production rates.

As mentioned in the previous section, both comets were a factor of 2–3 more productive before perihelion than after, although both showed generally similar heliocentric distance dependencies before and after perihelion. Because of the size of the SWAN instrument field of view, we are limited to extracting nothing shorter than daily-average values of the production rate. Given typical rotation rates of comets then, we expect that the values are also rotationally averaged values. In the absence of any other complementary results at this point, the overall asymmetric production about perihelion likely points to a seasonal effect owing to the orientation of the spin axis as it varies with respect to the sun. The asymmetry could be due to either elongated nucleus shape or to the distribution of active regions on the surface.

There are a number of ongoing studies and surveys that examine the ratios of various comet gas species in order to classify comets into groups, and perhaps give clues to their location of origin in the solar system, or about their evolutionary history. The location of *SOHO* at the L1 point enables SWAN to provide useful measures of the activity on short day-to-day and long timescales, providing a true measure of the activity with orbital position, as well as providing a temporal context to most observing programs which have only limited and sporadic time coverage. Therefore, in addition to providing many water production rate values, we have been examining the variations of production rate over the whole orbit and classifying them according to the heliocentric distance power law. We have been comparing the absolute water production rate levels and

Table 4
C/2001 Q4 NEAT: Deconvolved Daily-Average Water Production Rates

ΔT (days)	Q (10^{28} s^{-1})	δQ (10^{28} s^{-1})
−212.029	1.818	1.7
−211.029	2.056	1.7
−180.029	5.091	3.9
−179.029	6.522	5.5
−178.029	6.090	4.8
−177.029	6.235	3.0
−172.029	9.609	7.2
−171.029	12.84	5.8
−168.029	8.064	2.9
−165.029	6.352	2.6
−163.029	5.712	6.7
−162.029	5.679	4.9
−153.029	8.487	8.1
−151.029	9.970	7.3
−150.029	12.12	3.4
−147.029	11.25	7.7
−129.029	15.10	10.
−126.029	15.33	12.
−125.029	15.71	12.
−124.029	16.71	10.
−123.029	18.11	8.4
−122.029	16.76	11.
−121.029	17.30	10.
−120.029	17.84	9.3
−119.029	18.08	10.
−118.029	18.68	9.1
−117.029	19.44	7.3
−116.029	19.00	1.1
−115.029	19.18	10.
−114.029	19.52	9.0
−113.029	20.15	9.6
−112.029	19.65	10.
−111.029	20.41	8.5
−110.029	20.47	14.
−109.029	20.91	13.
−108.029	21.76	11.
−107.029	20.16	18.
−106.029	21.42	15.
−105.029	23.36	11.
−104.029	21.89	11.
−103.029	24.86	9.1
−102.029	29.09	6.9
−101.029	23.42	11.
−100.029	24.78	9.3
−99.029	26.42	7.4
−98.029	24.39	8.4
−97.029	24.32	7.2
−96.029	24.26	5.9
−95.029	26.15	9.1
−94.029	26.40	7.5
−93.029	26.92	5.2
−92.029	26.91	9.6
−91.029	26.78	8.1
−90.029	26.81	6.3
−89.029	26.95	7.9
−88.029	27.86	9.3
−87.029	28.10	5.9
−86.029	28.55	7.1
−85.029	28.61	5.6
−84.029	28.30	3.7
−83.029	27.37	6.3
−82.029	27.24	5.4
−81.029	27.29	3.8
−80.029	31.40	7.9
−79.029	31.11	5.9
−78.029	30.67	4.6

Table 4
(Continued)

ΔT (days)	Q (10^{28} s^{-1})	δQ (10^{28} s^{-1})
−77.029	33.32	7.6
−76.029	35.28	8.4
−75.029	35.99	6.1
−74.029	34.49	10.
−73.029	35.40	8.4
−72.029	27.36	6.3
−71.029	27.22	5.2
−70.029	25.13	4.0
−69.029	25.15	3.2
−68.029	24.70	2.9
−67.029	24.50	2.3
−66.029	29.51	5.2
−65.029	29.12	3.5
−64.029	37.52	6.7
−63.029	39.31	2.8
−62.029	31.89	8.9
−61.029	32.05	6.4
−60.029	29.01	7.0
−59.029	28.73	4.7
−58.029	25.07	8.4
−57.029	24.35	6.4
−56.029	25.89	5.9
−55.029	24.86	3.4
−54.029	28.33	13.
−53.029	27.85	13.
−52.029	27.15	12.
−51.029	26.70	11.
−50.029	25.74	9.7
−49.029	24.69	8.3
−48.029	24.86	6.9
−47.029	25.09	5.7
−46.029	24.42	4.2
−45.029	24.83	3.5
−44.029	23.88	2.7
−43.029	23.15	1.8
−42.029	26.74	16
−41.029	33.97	0.53
−40.029	24.74	0.94
−39.029	40.07	7.9
−38.029	56.31	6.4
−37.029	73.44	14.
−36.029	68.40	7.1
−35.029	30.24	3.4
−33.029	38.29	1.3
−32.029	82.51	41.
−31.029	30.52	1.8
−30.029	27.97	1.7
−29.029	31.17	0.99
−24.029	23.25	2.8
−23.029	22.76	1.7
−22.029	22.90	1.2
−21.029	23.77	0.68
−20.029	27.16	0.376
−19.029	38.36	0.22
−18.029	39.38	0.26
−17.029	33.18	0.97
−16.029	31.21	0.75
−14.029	23.94	0.10
−12.029	29.56	1.7
−11.029	28.89	0.44
−10.029	38.53	0.49
−9.029	48.42	0.64
−8.029	40.48	0.12
−7.029	41.86	0.64
−6.029	24.48	2.7
−5.029	24.45	1.2

Table 4
(Continued)

ΔT (days)	Q (10^{28} s^{-1})	δQ (10^{28} s^{-1})
−4.029	29.28	0.57
−3.029	42.43	0.89
−2.029	22.32	1.4
−1.029	23.80	1.1
−0.029	30.19	0.75
0.971	20.39	0.83
1.971	20.78	0.56
2.971	27.60	0.72
3.971	21.41	1.9
4.971	21.45	1.53
5.971	21.55	0.78
6.971	21.12	0.80
7.971	24.29	1.0
8.971	18.63	2.7
9.971	18.50	1.5
10.971	19.41	0.79
11.971	18.14	2.1
12.971	19.05	1.6
13.971	20.95	1.2
14.971	19.98	1.6
15.971	21.51	1.1
16.971	20.26	1.5
17.971	22.56	1.4
18.971	17.62	3.6
19.971	18.62	7.0
20.971	18.97	3.0
21.971	18.26	7.0
22.971	18.29	3.1
23.971	18.59	8.7
24.971	19.15	4.5
25.971	17.47	10.
26.971	17.48	6.6
27.971	17.16	13.
28.971	17.13	9.6
29.971	16.75	13.
30.971	16.56	13.
39.971	16.19	1.5
40.971	16.08	11.
41.971	17.08	14.
42.971	17.38	9.5
43.971	17.02	12.
44.971	16.95	7.2
45.971	18.41	13.
46.971	18.51	10.
47.971	18.87	10.
48.971	18.62	6.9
49.971	21.23	6.2
50.971	21.33	3.4
51.971	23.31	10.
52.971	24.22	7.4
53.971	26.16	11.
54.971	27.91	11.
55.971	23.92	16.
56.971	25.84	16.
57.971	23.61	14.
58.971	24.62	13.
59.971	26.70	13.
60.971	23.55	12.
61.971	24.23	9.8
62.971	24.80	6.1
64.971	21.49	18
65.971	17.96	10.
66.971	15.91	7.6
67.971	14.68	5.6
68.971	14.18	3.9
69.971	14.53	6.8

Table 4
(Continued)

ΔT (days)	Q (10^{28} s^{-1})	δQ (10^{28} s^{-1})
70.971	13.64	6.0
71.971	13.35	4.5
72.971	12.11	6.6
73.971	12.00	4.5
74.971	12.52	2.8
75.971	11.21	7.2
76.971	11.24	6.6
77.971	11.36	5.6
78.971	11.02	6.3
79.971	11.30	5.6
80.971	11.71	4.6
81.971	10.32	6.4
82.971	10.20	6.3
83.971	10.20	5.9
84.971	9.364	6.4
85.971	9.148	6.2
86.971	9.153	5.5
87.971	8.909	5.8
88.971	8.820	5.5
89.971	9.006	4.6
90.971	8.284	6.1
91.971	8.263	5.6
92.971	8.407	4.7
93.971	7.799	6.8
94.971	8.017	6.2
95.971	8.466	5.3
96.971	7.530	6.7
97.971	7.890	6.0
98.971	8.584	5.0
99.971	7.936	5.7
100.971	8.202	5.2
101.971	9.007	4.4
102.971	6.718	6.4
103.971	7.148	5.9
104.971	6.899	5.3
105.971	6.313	6.0
106.971	6.103	5.4
107.971	6.156	4.1
114.971	5.585	5.5
115.971	6.111	5.0
116.971	6.744	3.9
117.971	5.785	4.2
118.971	5.966	4.6
119.971	6.632	4.1
120.971	6.953	4.2
121.971	7.466	4.0
122.971	8.485	3.7
123.971	7.114	4.2
124.971	7.317	4.2
125.971	7.523	4.2
126.971	7.712	4.1
127.971	7.922	4.2
128.971	8.135	4.3
129.971	6.904	3.7
130.971	6.744	3.6
131.971	6.600	3.6
132.971	6.476	3.3
133.971	6.177	3.6
134.971	7.938	3.4
135.971	7.162	3.2
136.971	6.636	2.8
137.971	6.376	2.3
138.971	5.445	3.1
139.971	5.022	3.1
140.971	5.169	3.5
141.971	5.158	3.5

Table 4
(Continued)

ΔT (days)	Q (10^{28} s^{-1})	δQ (10^{28} s^{-1})
142.971	5.374	3.2
143.971	5.737	2.7
144.971	4.876	3.8
145.971	4.840	3.7
146.971	5.205	3.5
147.971	4.420	3.7
148.971	4.648	3.5
149.971	4.978	3.0

Notes.
ΔT: time from perihelion 2004 May 15.97, in days.
Q: water production rate (10^{28} s^{-1}).
δQ: 1σ uncertainty (10^{28} s^{-1}).

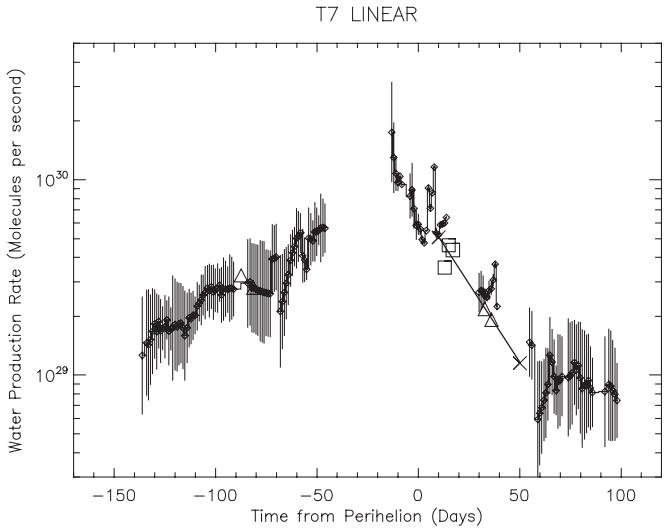

Figure 3. TRM deconvolved daily-average water production rate of C/2002 T7 (LINEAR) as a function of time. Shown as the diamonds connected by a histogram line are the daily-average water production rates of comet C/2002 T7 (LINEAR) determined with the time-resolved model from the SWAN images. The vertical lines correspond to the formal fitted model error bars. The large triangles are the Odin water production from Biver et al. (2007), the X's and line are from Anderson et al. (2008), and the squares are from DiSanti et al. (2006).

power-law slopes with various volatile composition measures elsewhere to look for any trends or correlations.

Five Oort Cloud comets, 1999 H1 Lee, 1999 T1 McNaught–Hartley, 2000 WM1 LINEAR, 2001 A2 LINEAR, and 2002 C1 Ikeya-Zhang (P153) were also observed with SWAN (Combi et al. 2008) and analyzed in the same way as Q4 and T7. These were compared with previous SWAN observations of 1996 B2 Hyakutake (Combi et al. 2005), 1999 S4 LINEAR (Mäkinen et al. 2001), 2006 P1 McNaught (Neugebauer et al. 2007), and Hale–Bopp (Combi et al. 2000, 2006). It was found that the comets fell into three groups according to their power-law slopes: (1) shallow with $p \sim -1.5$, (2) nominal ($-3 < p < -2$), and (3) steep ($p < -3.5$). This classification scheme would put T7 in the shallow group and Q4 in the nominal group. Table 5 gives an updated version of our summary of water production rates and power-law slopes for the SWAN comets published to date including Q4 and T7. In most of these comets, there were pre- to post-perihelion asymmetries in overall production level and some irregular variations owing to outbursts, e.g., for C/2000 A2 LINEAR (Combi et al. 2008), and seasonal effects from either the nucleus shape or the distribution of active areas, e.g.,

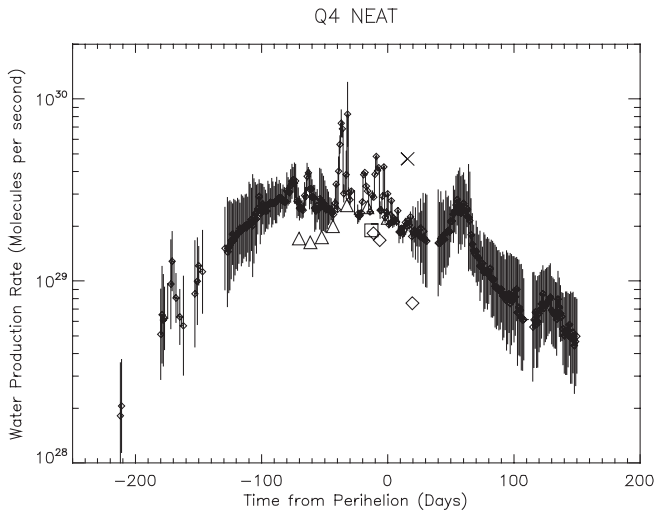

Figure 4. TRM deconvolved daily-average water production rate of C/2001 Q4 (NEAT) as a function of time. Shown as the diamonds connected by a histogram line are the daily-average water production rates of comet C/2001 Q4 (NEAT) determined with the time-resolved model from the SWAN images. The vertical lines correspond to the formal fitted model error bars. The large triangles are the Odin water production from Biver et al. (2007), the large diamonds are from J. Crovisier et al. (2009, in preparation), the X is from Anderson et al. (2008), and the large square is from Weaver et al. (2004).

for Hyakutake (Combi et al. 2005). However, with the advantage of having a consistent set of water production rate over a large portion of the apparition, our results are able to place peculiar variations (short and intermediate term) into proper context and reveal that the slopes of the underlying variations were generally similar for the same comet over the whole apparition.

T7 and Q4 were two moderately bright comets observed during the same general time period; a number of publications, like this one, have included observations of both and comparisons of them together and with other comets. Remijan et al. (2006), based on observations of several molecules including HCN and CH_3OH, concluded that T7 is compositionally similar to Hale–Bopp, while Q4 is more similar to Hyakutake, with T7 and Hale–Bopp being richer in HCN and CH_3OH compared to water and Q4 and Hyakutake being poorer in both. M. A. DiSanti et al. (2008, private communication) find that Q4 has abundances of CO and C_2H_6 relative to water of 3%–9% and ∼0.5%, respectively, and that T7 has abundances of these species of 2%–3% and ∼0.5%, respectively. In contrast, both Hale–Bopp and Hyakutake were much more enriched in CO, 23% and 19%–30%, respectively, compared with either Q4 or T7. Milam et al. (2006) find both T7 and Q4 depleted in formaldehyde, compared with Hale–Bopp, but similar to 1P/Halley. Lupu et al. (2007) find a CO production in Q4 relative to water of 8.8% ± 0.8% from *HST* observations. Finally, Gibb et al. (2007) find that CO and CH_4 do not correlate in a sample of eight comets including Q4 and T7. Table 5 gives an updated version of our summary of water production rate power-law slopes for the SWAN comets published to date compared with the abundances of CO and C_2H_6 compared with water.

4. SUMMARY

We present single-image values and sequences of daily-average values of the water production rate in comets C/2001 Q4 NEAT and C/2002 T7 LINEAR obtained by analysis of *SOHO* SWAN images of their H Lyα comae. The average power-law fit to the production rate variation of Q4 gives 3.5×10^{29} $r^{-1.7}$ and that for T7 gives 4.6×10^{29} $r^{-2.0}$. Q4 showed a very large production rate spike about 30 days before perihelion and then a large extended increase above the nominal trend from 50 to 70 days after perihelion. T7 showed no large outbursts. Both comets were more productive at comparable heliocentric distances before perihelion than after. In terms of the production

Table 5
Volatile Composition for Three Water Variation Groups in SWAN Comets

Comet	Q_1 (H_2O)[a]	p[b]	CO/H_2O	C_2H_6/H_2O
		Steep slope		
C 1999 T1 McNaught–Hartley[c]	2.9×10^{29}	−3.3	15% (1)	0.6% (2)
C 2001 A2 LINEAR[c]	8.2×10^{28}	−4.5	1.5% (1,3)	1.6% (3)
		Moderate slope		
C 1995 OI Hale–Bopp[d]	1.3×10^{31}	−2.6	23% (4,5)	0.6% (2)
C 1999 H1 Lee[c]	1.5×10^{29}	−2.7	2–4% (6,7)	0.7% (8)
P153/Ikeya-Zhang[c]	1.8×10^{29}	−2.7	4% (9,10)	0.6% (10)
C 1996 B2 Hyakutake[e]	2.7×10^{29}	−2.1	19–30% (11—14)	0.6% (15)
C 2002 T7 LINEAR[f]	$\mathbf{4.6\times10^{29}}$	−2.0	**2–3% (16)**	**∼0.5% (16)**
		Shallow slope		
C 1999 S4 LINEAR[g]	1.7×10^{28}	−1.6	0.6% (17,18)	0.1% (18)
C 2001 WM1 LINEAR[c]	1.1×10^{29}	−1.4	1% (1,9)	0.5% (19)
C 2006 P1 McNaught[h]	9.2×10^{29}	−1.7	2–4% (20)	—
C 2001 Q4 NEAT[f]	$\mathbf{3.5\times10^{29}}$	−1.7	**3–9% (16)**	**∼0.5% (16)**

Notes.
Note that the new results for T7 and Q4 are shown in **bold** type.
[a]Average pre-post water production rate at 1 AU in molecules s^{-1}.
[b]Average pre-post power-law exponent.
References for SWAN water production rates and slopes: [c]Combi et al. (2008); [d]Combi et al. (2000); [e]Combi et al. (2005); [f]This paper; [g]Mäkinen et al. (2001); [h]Neugebauer et al. (2007).
References for volatile abundances: (1) Biver et al. 2006; (2) Dello Russo et al. 2001; (3) Magee-Sauer et al. 2008; (4) DiSanti et al. 2001; (5) Bockelée-Morvan et al. 2000; (6) Biver et al. 2000; (7) Mumma et al. 2001a; (8) Mumma et al. 2001b; (9) Weaver et al. 2002; (10) DiSanti et al. 2002; (11) DiSanti et al. 2003; (12) McPhate et al. 1996; (13) Biver et al. 1999; (14) Lis et al. 1997; (15) Mumma et al. 1996; (16) M. A. DiSanti et al. 2008 (private communication); (17) Weaver et al. 2001; (18) Mumma et al. 2001a; (19) Radeva et al. 2008; (20) Dello Russo et al. 2007.

rate power-law slope classification by Combi et al. (2008), Q4 falls in the shallow slope group and T7 falls in the moderate slope group. So far our comparison of slopes and production rates level shows no obvious correlations with either CO or C_2H_6 abundance variations. In the future, we will expand our comparisons with other detected species as well as Afρ and the standard visual radical composition groups.

SOHO is an international cooperative mission between ESA and NASA. M. Combi acknowledges support from grants NNG05GF06G and NNG08A044G from the NASA Planetary Astronomy Program. J.-L. Bertaux and E. Quémerais acknowledge support from CNRS and CNES. J.T.T. Mäkinen was supported by the Finnish Meteorological Institute. We obtained cometary ephemerides from the JPL Horizons Web site. We also acknowledge the personnel that have been keeping *SOHO* and SWAN operational for 13 years. We thank Nathaniel Henry who helped with the data reduction. We also thank the referee, Lori Feaga, who made a number of helpful comments and criticisms that have greatly improved the paper.

REFERENCES

Anderson, W. M., DiSanti, M. A., Mumma, M. J., Bonev, B. P., Villaneuva, G. L., Dello Russo, N., Magee-Sauer, K., & Gibb, E. L. 2008, in LPI Contribution 1405, Asteroids, Comets, Meteors held 2008 July 14–18, Baltimore, MD, paper 8387
Bertaux, J.-L., et al. 1997, Solar Physics, 175, 737
Biver, N., et al. 1999, AJ, 118, 1850
Biver, N., et al. 2000, AJ, 120, 1554
Biver, N., et al. 2006, A&A, 449, 1255
Biver, N., et al. 2007, Planet. Space Sci., 55, 1058
Bockelée-Morvan, D., et al. 2000, A&A, 353, 1101
Combi, M. R., Mäkinen, J. T. T., Bertaux, J.-L., & Quémerais, E. 2005, Icarus, 177, 228
Combi, M. R., Mäkinen, J. T. T., Henry, N. J., Bertaux, J.-L., & Quémerais, E. 2006, BAAS, 38, 535
Combi, M. R., Mäkinen, J. T. T., Henry, N. J., Bertaux, J.-L., & Quémerais, E. 2008, AJ, 135, 1533
Combi, M. R., Reinard, A. A., Bertaux, J.-L., Quémerais, E., & Mäkinen, T. 2000, Icarus, 144, 191
Combi, M. R., & Smyth, W. H. 1988, ApJ, 327, 1044
Dello Russo, N., Mumma, M. J., DiSanti, M. A., Magee-Sauer, K., & Novak, R. 2001, Icarus, 153, 162
Dello Russo, N., Vervack, R. J. Jr., Weaver, H. A., & Lisse, C. M. 2007, BAAS, 39, 507
DiSanti, M. A., Bonev, B. P., Magee-Sauer, K., Dello Russo, N., Mumma, M. J., Reuter, D. C., & Villanueva, G. L. 2006, ApJ, 650, 470
DiSanti, M. A., Dello Russo, N., Magee-Sauer, K., Gibb, E. L., Reuter, D. C., & Mumma, M. J. 2002, in Proc. Asteroids Comets Meteors 2002, ed. B. Warmbein (ESA SP-5000; Noordwijk: ESA), 571
DiSanti, M. A., Mumma, M. J., Dello Russo, N., & Magee-Sauer, K. 2001, Icarus, 153, 361
DiSanti, M. A., Mumma, M. J., Dello Russo, N., Magee-Sauer, K., & Griep, D. 2003, J. Geophys. Res., 108, 5061
Festou, M. C. 1981, A&A, 95, 69
Gibb, E., Bonev, B. P., Mumma, M. J., DiSanti, M. A., Magee-Sauer, K., & Villanueva, G. 2007, BAAS, 38, 522
Keller, H. U., & Meier, R. R. 1976, A&A, 52, 273
Lis, D. C., et al. 1997, Earth Moon Planets, 87, 13
Lupu, R. E., Feldman, P. D., Weaver, H. A., & Tozzi, G.-P. 2007, ApJ, 670, 1473
Magee-Sauer, K., Mumma, M. J., DiSanti, M. A., Dello Russo, N., Gibb, E. L., & Bonev, B. P. 2008, Icarus, 194, 347
Mäkinen, J. T. T., Bertaux, J.-L., Combi, M. R., & Quémerais, E. 2001, Science, 292, 1326
Mäkinen, J. T. T., Bertaux, J.-L., Combi, M. R., & Quémerais, E. 2007, Icarus, 187, 109
Mäkinen, J. T. T., & Combi, M. R. 2005, Icarus, 177, 217
McPhate, J. B., Feldman, P. D., Weaver, H. A., A'Hearn, M. F., Tozzi, G.-P., & Festou, M. C. 1996, BAAS, 28, 1093
Milam, S. N., et al. 2006, ApJ, 649, 1169
Mumma, M. J., DiSanti, M. A., Dello Russo, N., Fomenkova, M., Magee-Sauer, K., Kaminski, C. D., & Xie, D. X. 1996, Science, 272, 1310
Mumma, M. J., et al. 2001a, Science, 292, 1334
Mumma, M. J., et al. 2001b, ApJ, 546, 1183
Neugebauer, M., et al. 2007, ApJ, 667, 1262
Radeva, Y. L., Mumma, M. J., Bonev, B. P., DiSanti, M. A., Villanueva, G. L. B. P., Magee-Sauer, K., Gibb, E. L., & Weaver, H. A. 2008, BAAS, 40, 416
Remijan, A. J., et al. 2006, ApJ, 643, 567
Schleicher, D. G., Woodney, L. M., & Millis, R. L. 2003, Icarus, 162, 415
Weaver, H. A., A'Hearn, M. F., Arpigny, C., Combi, M. R., Feldman, P. D., Festou, M. C., & Tozzi, G.-P. 2004, BAAS, 36, 1120
Weaver, H., Feldman, P. D., Combi, M. R., Krasnopolsky, V., Lisse, C. M., & Shemansky, D. E. 2002, ApJ, 576, L95
Weaver, H. A., et al. 2001, Science, 292, 1329
Yoshida, S. 2008, MISAO Project Comet Catalog, http://www.aerith.net/comet/catalog/index-T-earth.html